

## Electronic Supplementary Material (ESI)

### Understanding Trends in Activity and Selectivity of Bi-atom Catalysts for Electrochemical Reduction of Carbon Dioxide

Fuhua Li and Qing Tang\*

School of Chemistry and Chemical Engineering, Chongqing Key Laboratory of  
Theoretical and Computational Chemistry, Chongqing University, Chongqing 401331,  
China

\*To whom correspondence should be addressed. E-mail: qingtang@cqu.edu.cn.

Table S1. The distances between the central metal atoms ( $d_{M-M}$ ) in homo-nuclear BACs and the distance between two adjacent atoms in bulk metal ( $b_{M-M}$ ), unit in angstrom (Å).

Species	Bulk	BACs
Ag	2.89	2.77
Al	2.86	2.59
Au	2.88	2.70
Ca	3.95	3.08
Co	2.50	2.25
Cr	2.50	2.28
Cu	2.56	2.62
Fe	2.48	2.22
Hf	3.13	2.98
Ir	2.72	2.38
Mg	3.20	2.63
Mo	2.73	2.38
Nb	2.86	2.54
Ni	2.49	2.57
Os	2.68	2.35
Pd	2.75	2.63
Pt	2.78	2.69
Re	2.74	2.35
Rh	2.69	2.36

Ru	2.65	2.33
Sc	3.25	2.95
Sn	2.81	3.40
Sr	4.30	3.27
Ta	2.86	2.59
Ti	2.89	2.61
W	2.74	2.41
Y	3.56	3.26
Zn	2.67	2.57
Zr	3.18	2.96
Mn	2.28	2.27
Ga	2.53	2.67
Bi	3.10	3.45

Table S2. The number of electrons ( $n_e$ ) involved in the dissolution for the pure metals, standard dissolution potentials ( $U_{\text{diss(metal)}}^0$ , pH = 0), energy of central metal atom ( $E_M$ ), the formation energy,  $E_f$ , and computed dissolution potentials ( $U_{\text{diss}}$ ) for SACs. Some of them refers from the publication of Guo et al.<sup>1</sup>

Species	$n_e$	$U_{\text{diss(metal)}}^0$ (V)	$E_M$ (eV)	$E_f$ (eV)	$U_{\text{diss}}$ (V)
Ag	1	0.80	-2.83	-0.23	1.03
Al	3	-1.66	-3.75	-5.04	0.02
Au	3	1.50	-3.90	-0.09	1.53
Bi	1	0.50	-3.90	-1.58	2.08
Ca	2	-2.89	-1.96	-4.36	-0.71
Co	2	-0.28	-7.11	-3.39	1.41
Cr	2	-0.91	-9.64	-3.67	0.92
Cu	2	0.34	-4.10	-1.69	1.19
Fe	2	-0.45	-8.46	-3.50	1.30

---

Ga	3	-0.55	-3.04	-2.58	0.31
Hf	4	-1.55	-9.95	-4.20	-0.50
Ir	3	1.16	-8.86	-2.38	1.95
Mg	2	-2.37	-0.55	-4.78	0.02
Mn	2	-1.19	-9.16	-3.96	0.79
Mo	3	-0.20	-10.86	-2.41	0.60
Nb	3	-1.10	-10.11	-3.27	-0.01
Ni	2	-0.26	-5.78	-2.95	1.22
Os	8	0.84	-11.22	-2.20	1.11
Pd	2	0.95	-5.18	-2.06	1.98
Pt	2	1.18	-6.06	-2.11	2.24
Re	3	0.30	-12.44	-2.15	1.02
Rh	2	0.60	-7.36	-2.76	1.98
Ru	2	0.46	-9.28	-2.65	1.78
Sc	3	-2.08	-6.34	-5.31	-0.31
Sn	2	-0.14	-4.01	-2.12	0.92
Sr	2	-2.90	-1.69	-8.62	1.41
Ta	3	-0.60	-11.86	-2.88	0.36
Ti	2	-1.63	-7.90	-4.32	0.53
V	2	-1.18	-9.09	-3.73	0.68
W	3	0.10	-12.96	-2.44	0.91
Y	3	-2.37	-6.47	-7.33	0.07

---

Zn	2	-0.76	-1.27	-2.16	0.32
Zr	4	-1.45	-8.55	-3.90	-0.48

Table S3. The detailed electronic energy ( $E^*$ ) and binding energy ( $E$ ) of critical intermediates ( $^*CO_2$ ,  $^*COOH$ ,  $^*CO$ , and  $^*HCOO$ ) in homonuclear BACs during electrochemical  $CO_2RR$ .

Species	$E^*$	$E_{^*CO_2}$	$E_{CO_2}$	$E_{^*COOH}$	$E_{COOH}$	$E_{^*CO}$	$E_{CO}$	$E_{^*HCOO}$	$E_{HCOO}$
Bi-Bi	-513.98	-537.05	-0.11	-539.23	0.90	-528.85	0.21	-539.89	-0.21
Co-Co	-524.01	-547.09	-0.12	-549.87	0.30	-538.89	0.19	-549.55	0.46
Cr-Cr	-529.64	-552.73	-0.13	-556.79	-1.00	-545.98	-1.27	-556.83	-1.72
Cu-Cu	-514.60	-537.78	-0.22	-539.71	1.04	-529.48	0.20	-540.04	0.51
Fe-Fe	-526.94	-550.02	-0.13	-553.23	-0.13	-542.46	-0.45	-552.87	-0.21
Ga-Ga	-514.30	-537.41	-0.15	-541.04	-0.59	-529.31	0.07	-541.70	-1.64
Ir-Ir	-525.50	-548.62	-0.16	-551.46	0.19	-540.21	0.36	-550.72	1.01
MnMn	-529.26	-552.33	-0.11	-555.94	-0.53	-545.38	-1.05	-555.84	-0.72
MoMo	-529.56	-552.61	-0.10	-556.66	-0.95	-546.11	-1.48	-557.36	-2.63
Ni-Ni	-520.48	-543.57	-0.13	-545.81	0.83	-535.36	0.20	-545.75	0.93
Os-Os	-529.85	-552.96	-0.16	-556.77	-0.77	-545.98	-1.05	-556.13	1.01
Pd-Pd	-517.50	-540.81	-0.36	-543.22	0.43	-532.57	0.00	-542.61	0.91
Pt-Pt	-519.36	-542.70	-0.39	-545.30	0.22	-534.46	-0.03	-544.40	1.04
Re-Re	-532.17	-555.26	-0.12	-559.01	-0.68	-548.92	-1.67	-559.27	-0.31
Rh-Rh	-523.25	-546.35	-0.14	-548.84	0.56	-538.13	0.20	-548.52	1.03
Ru-Ru	-526.87	-549.98	-0.15	-553.65	-0.62	-542.78	-0.83	-553.15	0.09

Sn-Sn	-515.29	-538.35	-0.11	-541.39	0.05	-530.13	0.23	-541.78	-0.14
Sr-Sr	-524.23	-547.51	-0.33	-549.92	0.46	-539.27	0.03	-551.25	-1.40
Ta-Ta	-532.50	-557.13	-1.67	-560.22	-1.57	-549.02	-1.44	-561.58	-4.06
Ti-Ti	-527.46	-551.27	-0.85	-554.67	-1.05	-543.47	-0.93	-556.11	-3.57
V-V	-528.66	-551.85	-0.24	-555.55	-0.74	-544.83	-1.10	-556.80	-3.19
W-W	-533.81	-556.88	-0.12	-560.49	-0.52	-549.76	-0.88	-561.27	-2.14
Zn-Zn	-509.88	-532.96	-0.12	-535.59	0.44	-524.73	0.22	-536.06	-0.40
Ag-Ag	-509.14								
Al-Al	-520.60								
Au-Au	-511.00								
Ca-Ga	-515.65								
Hf-Hf	-531.33								
MgMg	-513.68								
Nb-Nb	-529.77								
Sc-Sc	-526.32								
Y-Y	-530.61								
Zr-Zr	-527.91								

Table S4. The detailed electronic energy ( $E^*$ ) and binding energy ( $E$ ) of critical intermediates ( $^*CO_2$ ,  $^*COOH$ ,  $^*CO$ ,  $^*H$ , and  $^*HCOO$ ) in Mo-based heteronuclear BACs during electrochemical  $CO_2RR$ .

Species	Mo-Fe	Mo-Co	Mo-Ir	Mo-Rh	Mo-Ni	Mo-Cu	Mo-Zn	Mo-Ga
$E^*$	-528.60	-527.34	-528.41	-527.17	-525.25	-522.24	-520.01	-521.30

$E^*_{\text{CO}_2}$	-552.32	-550.52	-551.50	-550.26	-548.32	-545.31	-543.23	-545.26
$E_{\text{CO}_2}$	-0.76	-0.23	-0.13	-0.13	-0.11	-0.11	-0.26	-1.00
$E^*_{\text{COOH}}$	-555.45	-553.26	-554.37	-552.72	-550.65	-548.15	-546.62	-548.11
$E_{\text{COOH}}$	-0.70	0.23	0.20	0.60	0.76	0.25	-0.46	-0.65
$E^*_{\text{CO}}$	-545.16	-543.94	-544.98	-543.74	-541.96	-538.95	-536.67	-537.90
$E_{\text{CO}}$	-1.48	-1.53	-1.50	-1.50	-1.63	-1.63	-1.59	-1.51
$E^*_{\text{H}}$	-532.59	-531.49	-532.54	-531.31	-529.44	-526.42	-524.13	-525.35
$E_{\text{H}}$	-0.54	-0.71	-0.69	-0.69	-0.74	-0.73	-0.68	-0.59
$E^*_{\text{HCOO}}$	-556.41	-555.16	-556.17	-554.97	-553.09	-550.05	-548.07	-549.63
$E_{\text{HCOO}}$	-1.65	-1.67	-1.61	-1.64	-1.68	-1.65	-1.91	-2.17

Table S5. The detailed electronic energy ( $E^*$ ) and binding energy ( $E$ ) of critical intermediates ( $^*\text{CO}_2$ ,  $^*\text{COOH}$ ,  $^*\text{CO}$ ,  $^*\text{H}$ , and  $^*\text{HCOO}$ ) in Ta-based heteronuclear BACs during electrochemical  $\text{CO}_2\text{RR}$ .

Species	Ta-Fe	Ta-Co	Ta-Ir	Ta-Rh	Ta-Ni	Ta-Cu	Ta-Zn	Ta-Ga
$E^*$	-530.26	-529.04	-530.08	-528.89	-527.40	-524.33	-522.05	-523.37
$E^*_{\text{CO}_2}$	-555.00	-553.49	-554.35	-553.14	-551.98	-548.93	-546.63	-548.28
$E_{\text{CO}_2}$	-1.79	-1.50	-1.31	-1.30	-1.63	-1.64	-1.62	-1.95
$E^*_{\text{COOH}}$	-558.23	-556.09	-556.93	-555.51	-553.46	-551.29	-549.28	-550.89
$E_{\text{COOH}}$	-1.82	-0.89	-0.69	-0.47	0.29	-0.81	-1.07	-1.36
$E^*_{\text{CO}}$	-546.77	-545.69	-546.80	-545.56	-543.91	-540.90	-538.64	-539.96
$E_{\text{CO}}$	-1.44	-1.57	-1.64	-1.59	-1.43	-1.49	-1.51	-1.51
$E^*_{\text{H}}$	-534.89	-533.68	-534.66	-533.44	-532.06	-528.98	-526.66	-527.93

$E_H$	-1.19	-1.19	-1.12	-1.10	-1.22	-1.20	-1.16	-1.11
$E_{*HCOO}$	-559.22	-558.05	-559.02	-557.82	-556.39	-553.29	-550.93	-552.51
$E_{HCOO}$	-2.81	-2.86	-2.78	-2.77	-2.84	-2.80	-2.73	-2.99

Table S6. The detailed electronic energy ( $E^*$ ) and binding energy ( $E$ ) of critical intermediates ( $*CO_2$ ,  $*COOH$ ,  $*CO$ ,  $*H$ , and  $*HCOO$ ) in V-based heteronuclear BACs during electrochemical  $CO_2RR$ .

Species	V-Fe	V-Co	V-Ir	V-Rh	V-Ni	V-Cu	V-Zn	V-Ga
$E^*$	-528.40	-527.11	-528.09	-526.82	-525.46	-522.25	-519.85	-521.41
$E_{*CO_2}$	-552.25	-550.86	-551.78	-550.48	-548.54	-545.31	-542.94	-545.31
$E_{CO_2}$	-0.89	-0.79	-0.73	-0.70	-0.12	0.10	-0.13	-0.94
$E_{*COOH}$	-555.76	-553.71	-554.64	-553.21	-551.20	-548.14	-546.57	-548.51
$E_{COOH}$	-1.21	-0.45	-0.39	-0.23	0.61	0.47	-0.56	-0.94
$E_{*CO}$	-544.52	-543.47	-544.46	-543.16	-541.62	-538.45	-536.07	-537.60
$E_{CO}$	-1.05	-1.28	-1.29	-1.26	-1.08	-1.12	-1.14	-1.11
$E_{*H}$	-532.00	-530.78	-531.70	-530.43	-529.17	-525.94	-523.52	-525.08
$E_H$	-0.15	-0.22	-0.17	-0.16	-0.26	-0.24	-0.22	-0.22
$E_{*HCOO}$	-556.45	-554.82	-555.78	-554.54	-553.24	-550.06	-548.03	-550.04
$E_{HCOO}$	-1.89	-1.56	-1.53	-1.56	-1.63	-1.65	-2.03	-2.48

Table S7. The detailed electronic energy ( $E^*$ ) and binding energy ( $E$ ) of critical intermediates ( $*CO_2$ ,  $*COOH$ ,  $*CO$ ,  $*H$ , and  $*HCOO$ ) in Ti-based heteronuclear BACs during electrochemical  $CO_2RR$ .

Species	Ti-Fe	Ti-Co	Ti-Ir	Ti-Rh	Ti-Ni	Ti-Cu	Ti-Zn	Ti-Ga
---------	-------	-------	-------	-------	-------	-------	-------	-------

$E^*$	-527.65	-526.44	-527.47	-526.20	-524.82	-521.65	-519.31	-520.88
$E^*_{\text{CO}_2}$	-551.90	-550.64	-551.55	-550.25	-548.30	-545.17	-542.83	-545.19
$E_{\text{CO}_2}$	-1.30	-1.25	-1.12	-1.09	-0.52	-0.57	-0.56	-1.35
$E^*_{\text{COOH}}$	-555.39	-553.70	-554.67	-553.22	-551.01	-548.03	-546.29	-548.53
$E_{\text{COOH}}$	-1.59	-1.11	-1.04	-0.86	0.17	-0.23	-0.83	-1.50
$E^*_{\text{CO}}$	-543.54	-542.36	-543.35	-542.09	-540.83	-537.65	-535.32	-537.04
$E_{\text{CO}}$	-0.82	-0.85	-0.80	-0.81	-0.93	-0.93	-0.94	-1.09
$E^*_{\text{H}}$	-531.15	-529.99	-530.94	-529.61	-528.56	-525.37	-523.02	-524.91
$E_{\text{H}}$	-0.06	-0.10	-0.02	0.04	-0.29	-0.27	-0.27	-0.59
$E^*_{\text{HCOO}}$	-555.74	-554.57	-555.56	-554.34	-553.15	-549.99	-547.84	-550.09
$E_{\text{HCOO}}$	-1.89	-1.56	-1.53	-1.56	-1.63	-1.65	-2.03	-2.48

Table S8. The detailed electronic energy ( $E^*$ ) and binding energy ( $E$ ) of critical intermediates ( $^*\text{CO}_2$ ,  $^*\text{COOH}$ ,  $^*\text{CO}$ ,  $^*\text{H}$ , and  $^*\text{HCOO}$ ) in Cr-based heteronuclear BACs during electrochemical  $\text{CO}_2\text{RR}$ .

Species	Cr-Fe	Cr-Co	Cr-Ir	Cr-Rh	Cr-Ni	Cr-Cu	Cr-Zn	Cr-Ga
$E^*$	-528.19	-526.94	-527.81	-526.56	-524.73	-521.57	-519.20	-521.30
$E^*_{\text{CO}_2}$	-551.38	-550.04	-550.92	-549.67	-547.83	-544.67	-542.30	-544.41
$E_{\text{CO}_2}$	-0.23	-0.14	-0.15	-0.14	-0.14	-0.14	-0.14	-0.15
$E^*_{\text{COOH}}$	-554.77	-552.72	-553.73	-552.32	-549.94	-546.68	-545.34	-548.00
$E_{\text{COOH}}$	-0.43	0.37	0.23	0.40	0.95	1.05	0.01	-0.54
$E^*_{\text{CO}}$	-544.63	-543.49	-544.41	-543.12	-541.52	-538.29	-535.88	-537.47
$E_{\text{CO}}$	-1.05	-0.88	-0.91	-0.89	-0.88	-0.91	-1.00	-0.87



$E_{*H}$	-532.04	-530.88	-531.81	-530.53	-528.89	-525.65	-523.21	-524.66
$E_H$	-0.10	0.10	0.06	0.07	0.12	0.10	0.05	0.31
$E_{*HCOO}$	-555.99	-554.40	-555.23	-553.98	-552.52	-549.32	-547.44	-549.59
$E_{HCOO}$	-1.34	-0.71	-0.66	-0.67	-0.80	-0.86	-1.47	-1.91

Table S9. The detailed electronic energy ( $E^*$ ) and binding energy ( $E$ ) of critical intermediates ( $*CO_2$ ,  $*COOH$ ,  $*CO$ ,  $*H$ , and  $*HCOO$ ) in Mn-based heteronuclear BACs during electrochemical  $CO_2RR$ .

Species	Mn-Fe	Mn-Co	Mn-Ir	Mn-Rh	Mn-Ni	Mn-Cu	Mn-Zn	Mn-Ga
$E^*$	-528.19	-526.94	-527.81	-526.56	-524.73	-521.57	-519.20	-521.30
$E_{*CO_2}$	-551.38	-550.04	-550.92	-549.67	-547.83	-544.67	-542.30	-544.41
$E_{CO_2}$	-0.23	-0.14	-0.15	-0.14	-0.14	-0.14	-0.14	-0.15
$E_{*COOH}$	-554.77	-552.72	-553.73	-552.32	-549.94	-546.68	-545.34	-548.00
$E_{COOH}$	-0.43	0.37	0.23	0.40	0.95	1.05	0.01	-0.54
$E_{*CO}$	-544.11	-542.77	-543.58	-542.38	-540.65	-537.38	-535.04	-537.05
$E_{CO}$	-0.85	-0.75	-0.70	-0.74	-0.84	-0.74	-0.76	-0.67
$E_{*H}$	-531.49	-530.14	-531.01	-529.75	-528.01	-524.75	-522.38	-524.47
$E_H$	0.15	0.25	0.24	0.26	0.17	0.27	0.27	0.28
$E_{*HCOO}$	-554.91	-553.28	-554.08	-552.84	-551.35	-548.23	-546.46	-549.04
$E_{HCOO}$	-0.56	-0.19	-0.12	-0.12	-0.46	-0.51	-1.11	-1.58

Table S10. The detailed electronic energy ( $E^*$ ), zero-point energy ( $E_{ZPE}$ ), entropy corrections ( $TS$ ), free energy ( $G$ ), and Gibbs free energy change ( $\Delta G$ ) of critical intermediate in Mo-based

heteronuclear BACs during electrochemical CO<sub>2</sub>RR towards C1 product and competitive HER product.

Species	$E^*$	$E^*_{\text{CO}_2}$	$E_{\text{ZPE}}$	TS	$G$	$\Delta G$	$E^*_{\text{COOH}}$	$E_{\text{ZPE}}$	TS	$G$	$\Delta G$
Mo-Fe	-528.60	-552.32	0.32	0.14	-552.15	-0.33	-555.45	0.64	0.16	-554.98	0.36
Mo-Co	-527.34	-550.52	0.32	0.16	-550.36	0.18	-553.26	0.62	0.18	-552.81	0.75
Mo-Ir	-528.41	-551.50	0.32	0.23	-551.41	0.20	-554.37	0.62	0.17	-553.91	0.70
Mo-Rh	-527.17	-550.26	0.32	0.24	-550.18	0.19	-552.72	0.63	0.16	-552.25	1.13
Mo-Ni	-525.25	-548.32	0.30	0.19	-548.21	0.25	-550.65	0.61	0.12	-550.17	1.24
Mo-Cu	-522.24	-545.31	0.29	0.18	-545.20	0.25	-548.15	0.62	0.17	-547.69	0.70
Mo-Zn	-520.01	-543.23	0.29	0.15	-543.09	0.13	-546.62	0.63	0.17	-546.16	0.12
Mo-Ga	-521.30	-545.26	0.31	0.15	-545.10	-0.59	-548.11	0.63	0.17	-547.65	0.65
		$E^*_{\text{CO}}$	$E_{\text{ZPE}}$	TS	$G$	$\Delta G$	$E^*_{\text{HCOO}}$	$E_{\text{ZPE}}$	TS	$G$	$\Delta G$
Mo-Fe		-545.16	0.21	0.13	-545.08	-0.99	-556.41	0.61	0.15	-555.96	-0.36
Mo-Co		-543.94	0.20	0.13	-543.87	-1.94	-555.16	0.61	0.23	-554.78	-0.98
Mo-Ir		-544.98	0.21	0.13	-544.90	-1.88	-556.17	0.60	0.24	-555.80	-0.94
Mo-Rh		-543.74	0.20	0.14	-543.68	-2.32	-554.97	0.61	0.22	-554.58	-0.95
Mo-Ni		-541.96	0.32	0.14	-541.78	-2.49	-553.09	0.61	0.23	-552.71	-1.05
Mo-Cu		-538.95	0.20	0.15	-538.89	-2.09	-550.05	0.60	0.18	-549.63	-0.98
Mo-Zn		-536.67	0.21	0.13	-536.60	-1.32	-548.07	0.64	0.17	-547.60	-1.07
Mo-Ga		-537.90	0.20	0.13	-537.82	-1.06	-549.63	0.65	0.15	-549.14	-0.59
		$E^*_{\text{HCOOH}}$	$E_{\text{ZPE}}$	TS	$G$	$\Delta G$					
Mo-Fe		-559.17	0.93	0.24	-558.48	0.92					
Mo-Co		-557.82	0.92	0.25	-557.14	1.09					
Mo-Ir		-558.89	0.92	0.26	-558.22	1.02					
Mo-Rh		-557.70	0.92	0.24	-557.02	1.01					
Mo-Ni		-555.80	0.92	0.25	-555.13	1.03					
Mo-Cu		-552.61	0.92	0.25	-551.94	1.13					
Mo-Zn		-550.29	0.92	0.27	-549.64	1.40					
Mo-Ga		-552.49	0.93	0.28	-551.83	0.75					
		$E^*_{\text{H}}$	$E_{\text{ZPE}}$	TS	$G$	$\Delta G$	$E^*_{\text{H}_2}$	$E_{\text{ZPE}}$	TS	$G$	$\Delta G$
Mo-Fe		-532.59	0.18	0.02	-532.42	-0.37	-535.35	0.29	0.17	-535.23	0.64
Mo-Co		-531.49	0.18	0.01	-531.32	-0.54	-534.09	0.31	0.18	-533.96	0.82
Mo-Ir		-532.54	0.19	0.01	-532.37	-0.52	-535.16	0.31	0.19	-535.04	0.78
Mo-Rh		-531.31	0.18	0.01	-531.14	-0.52	-533.92	0.31	0.19	-533.80	0.79
Mo-Ni		-529.44	0.18	0.01	-529.27	-0.57	-532.01	0.32	0.02	-531.71	1.01
Mo-Cu		-526.42	0.15	0.01	-526.27	-0.58	-528.99	0.37	0.11	-528.73	0.99
Mo-Zn		-524.13	0.18	0.01	-523.96	-0.51	-526.77	0.27	0.07	-526.57	0.85
Mo-Ga		-525.35	0.18	0.02	-525.18	-0.43	-528.06	0.30	0.14	-527.90	0.73

Table S11. The detailed electronic energy ( $E^*$ ), zero-point energy ( $E_{\text{ZPE}}$ ), entropy corrections (TS),

free energy ( $G$ ), and Gibbs free energy change ( $\Delta G$ ) of critical intermediate in Ta-based heteronuclear BACs during electrochemical CO<sub>2</sub>RR towards C1 product and competitive HER product.

Species	$E^*$	$E^*_{\text{CO}_2}$	$E_{\text{ZPE}}$	TS	$G$	$\Delta G$	$E^*_{\text{COOH}}$	$E_{\text{ZPE}}$	TS	$G$	$\Delta G$
Ta-Fe	-530.26	-555.00	0.31	0.16	-554.85	-1.39	-558.23	0.63	0.17	-557.77	0.28
Ta-Co	-529.04	-553.49	0.31	0.17	-553.35	-1.10	-556.09	0.61	0.19	-555.66	0.88
Ta-Ir	-530.08	-554.35	0.32	0.15	-554.17	-0.88	-556.93	0.64	0.16	-556.46	0.91
Ta-Rh	-528.89	-553.14	0.32	0.15	-552.97	-0.87	-555.51	0.63	0.16	-555.05	1.12
Ta-Ni	-527.40	-551.98	0.30	0.19	-551.86	-1.26	-553.46	0.63	0.16	-552.99	2.07
Ta-Cu	-524.33	-548.93	0.30	0.19	-548.82	-1.28	-551.29	0.62	0.17	-550.84	1.18
Ta-Zn	-522.05	-546.63	0.30	0.18	-546.51	-1.25	-549.28	0.62	0.18	-548.84	0.87
Ta-Ga	-523.37	-548.28	0.30	0.16	-548.14	-1.56	-550.89	0.63	0.18	-550.44	0.89
		$E^*_{\text{CO}}$	$E_{\text{ZPE}}$	TS	$G$	$\Delta G$	$E^*_{\text{HCOO}}$	$E_{\text{ZPE}}$	TS	$G$	$\Delta G$
Ta-Fe		-546.77	0.19	0.10	-546.69	0.19	-559.22	0.63	0.14	-558.73	-0.43
Ta-Co		-545.69	0.19	0.09	-545.59	-0.81	-558.05	0.60	0.25	-557.71	-0.91
Ta-Ir		-546.80	0.19	0.16	-546.76	-1.19	-559.02	0.61	0.23	-558.64	-1.02
Ta-Rh		-545.56	0.19	0.15	-545.52	-1.36	-557.82	0.60	0.24	-557.45	-1.04
Ta-Ni		-543.91	0.20	0.14	-543.86	-1.75	-556.39	0.61	0.24	-556.02	-0.71
Ta-Cu		-540.90	0.23	0.15	-540.82	-0.86	-553.29	0.61	0.24	-552.93	-0.66
Ta-Zn		-538.64	0.19	0.04	-538.49	-0.54	-550.93	0.63	0.18	-550.47	-0.51
Ta-Ga		-539.96	0.19	0.09	-539.86	-0.30	-552.51	0.64	0.16	-552.03	-0.45
		$E^*_{\text{HCOOH}}$	$E_{\text{ZPE}}$	TS	$G$	$\Delta G$					
Ta-Fe		-561.63	0.91	0.25	-560.97	1.21					
Ta-Co		-560.43	0.91	0.24	-559.76	1.40					
Ta-Ir		-561.52	0.93	0.24	-560.84	1.25					
Ta-Rh		-560.31	0.92	0.25	-559.63	1.27					
Ta-Ni		-558.65	0.90	0.25	-558.00	1.47					
Ta-Cu		-555.57	0.88	0.20	-554.89	1.49					
Ta-Zn		-553.28	0.91	0.24	-552.61	1.31					
Ta-Ga		-554.44	0.89	0.14	-553.69	1.79					
		$E^*_{\text{H}}$	$E_{\text{ZPE}}$	TS	$G$	$\Delta G$	$E^*_{\text{H}_2}$	$E_{\text{ZPE}}$	TS	$G$	$\Delta G$
Ta-Fe		-534.89	0.18	0.02	-534.73	-1.03	-537.11	0.29	0.11	-536.93	1.25
Ta-Co		-533.68	0.18	0.02	-533.52	-1.03	-535.79	0.32	0.15	-535.63	1.34
Ta-Ir		-534.66	0.18	0.01	-534.49	-0.96	-536.84	0.30	0.14	-536.69	1.25
Ta-Rh		-533.44	0.18	0.01	-533.28	-0.94	-535.65	0.31	0.14	-535.48	1.25
Ta-Ni		-532.06	0.18	0.02	-531.90	-1.05	-534.15	0.32	0.16	-533.99	1.35
Ta-Cu		-528.98	0.18	0.01	-528.81	-1.03	-531.08	0.33	0.16	-530.92	1.34
Ta-Zn		-526.66	0.18	0.02	-526.50	-1.00	-528.80	0.31	0.17	-528.66	1.29
Ta-Ga		-527.93	0.18	0.02	-527.77	-0.95	-530.12	0.30	0.19	-530.01	1.21

Table S12. The detailed electronic energy ( $E^*$ ), zero-point energy ( $E_{ZPE}$ ), entropy corrections ( $TS$ ), free energy ( $G$ ), and Gibbs free energy change ( $\Delta G$ ) of critical intermediate in V-based heteronuclear BACs during electrochemical CO<sub>2</sub>RR towards C1 product and competitive HER product.

Species	$E^*$	$E^*_{CO_2}$	$E_{ZPE}$	TS	$G$	$\Delta G$	$E^*_{COOH}$	$E_{ZPE}$	TS	$G$	$\Delta G$
V-Fe	-528.40	-552.25	0.32	0.15	-552.08	-0.48	-555.76	0.64	0.15	-555.27	0.01
V-Co	-527.11	-550.86	0.32	0.11	-550.65	-0.34	-553.71	0.63	0.16	-553.24	0.61
V-Ir	-528.09	-551.78	0.33	0.16	-551.62	-0.32	-554.64	0.64	0.16	-554.15	0.66
V-Rh	-526.82	-550.48	0.33	0.15	-550.31	-0.28	-553.21	0.64	0.16	-552.73	0.78
V-Ni	-525.46	-548.54	0.32	0.23	-548.44	0.22	-551.20	0.57	0.22	-550.84	0.80
V-Cu	-522.25	-545.31	0.33	0.22	-545.21	0.25	-548.14	0.62	0.18	-547.70	0.70
V-Zn	-519.85	-542.94	0.28	0.17	-542.83	0.23	-546.57	0.62	0.18	-546.12	-0.09
V-Ga	-521.41	-545.31	0.31	0.15	-545.15	-0.53	-548.51	0.63	0.18	-548.06	0.29
		$E^*_{CO}$	$E_{ZPE}$	TS	$G$	$\Delta G$	$E^*_{HCOO}$	$E_{ZPE}$	TS	$G$	$\Delta G$
V-Fe		-544.52	0.20	0.14	-544.47	-0.09	-556.45	0.61	0.14	-555.98	-0.45
V-Co		-543.47	0.20	0.10	-543.38	-1.02	-554.82	0.62	0.19	-554.38	-0.28
V-Ir		-544.46	0.20	0.16	-544.42	-1.16	-555.78	0.61	0.22	-555.39	-0.33
V-Rh		-543.16	0.20	0.16	-543.12	-1.28	-554.54	0.60	0.24	-554.17	-0.41
V-Ni		-541.62	0.20	0.15	-541.57	-1.61	-553.24	0.61	0.22	-552.85	-0.96
V-Cu		-538.45	0.22	0.10	-538.33	-1.52	-550.06	0.61	0.22	-549.67	-1.02
V-Zn		-536.07	0.20	0.10	-535.97	-0.74	-548.03	0.63	0.19	-547.60	-1.32
V-Ga		-537.60	0.20	0.09	-537.50	-0.32	-550.04	0.64	0.17	-549.57	-0.97
		$E^*_{HCOOH}$	$E_{ZPE}$	TS	$G$	$\Delta G$					
V-Fe		-559.18	0.94	0.25	-558.50	0.93					
V-Co		-558.04	0.94	0.24	-557.34	0.49					
V-Ir		-559.07	0.94	0.23	-558.36	0.49					
V-Rh		-557.78	0.94	0.23	-557.07	0.55					
V-Ni		-556.01	0.93	0.25	-555.33	0.97					
V-Cu		-552.78	0.92	0.20	-552.06	1.06					
V-Zn		-550.40	0.92	0.20	-549.68	1.37					
V-Ga		-551.85	0.92	0.20	-551.13	1.89					
		$E^*_{H}$	$E_{ZPE}$	TS	$G$	$\Delta G$	$E^*_{H_2}$	$E_{ZPE}$	TS	$G$	$\Delta G$
V-Fe		-532.00	0.17	0.02	-531.84	0.00	-535.15	0.30	0.21	-535.05	0.24
V-Co		-530.78	0.18	0.02	-530.62	-0.06	-533.86	0.31	0.19	-533.74	0.33
V-Ir		-531.70	0.18	0.02	-531.54	-0.01	-534.85	0.32	0.15	-534.67	0.32
V-Rh		-530.43	0.17	0.02	-530.27	0.00	-533.58	0.32	0.16	-533.43	0.30
V-Ni		-529.17	0.18	0.01	-529.00	-0.10	-532.21	0.29	0.11	-532.03	0.42
V-Cu		-525.94	0.17	0.01	-525.78	-0.08	-528.98	0.28	0.09	-528.79	0.43
V-Zn		-523.52	0.17	0.02	-523.36	-0.07	-526.60	0.30	0.10	-526.40	0.41
V-Ga		-525.08	0.17	0.02	-524.92	-0.06	-528.17	0.30	0.13	-528.00	0.37

Table S13. The detailed electronic energy ( $E^*$ ), zero-point energy ( $E_{ZPE}$ ), entropy corrections (TS), free energy ( $G$ ), and Gibbs free energy change ( $\Delta G$ ) of critical intermediate in Ti-based heteronuclear BACs during electrochemical CO<sub>2</sub>RR towards C1 product and competitive HER product.

Species	$E^*$	$E^*_{CO_2}$	$E_{ZPE}$	TS	$G$	$\Delta G$	$E^*_{COOH}$	$E_{ZPE}$	TS	$G$	$\Delta G$
Ti-Fe	-527.65	-551.90	0.32	0.16	-551.74	-0.89	-555.39	0.64	0.16	-554.91	0.03
Ti-Co	-526.44	-550.64	0.32	0.17	-550.49	-0.85	-553.70	0.64	0.16	-553.23	0.46
Ti-Ir	-527.47	-551.55	0.33	0.15	-551.38	-0.69	-554.67	0.64	0.16	-554.18	0.40
Ti-Rh	-526.20	-550.25	0.32	0.17	-550.10	-0.69	-553.22	0.64	0.16	-552.74	0.56
Ti-Ni	-524.82	-548.30	0.29	0.23	-548.24	-0.21	-551.01	0.59	0.21	-550.63	0.81
Ti-Cu	-521.65	-545.17	0.32	0.09	-544.95	-0.09	-548.03	0.60	0.21	-547.65	0.50
Ti-Zn	-519.31	-542.83	0.29	0.23	-542.77	-0.25	-546.29	0.62	0.17	-545.84	0.13
Ti-Ga	-520.88	-545.19	0.30	0.16	-545.05	-0.96	-548.53	0.63	0.18	-548.08	0.16
		$E^*_{CO}$	$E_{ZPE}$	TS	$G$	$\Delta G$	$E^*_{HCOO}$	$E_{ZPE}$	TS	$G$	$\Delta G$
Ti-Fe		-543.54	0.18	0.17	-543.53	0.50	-555.81	0.63	0.17	-555.35	-0.16
Ti-Co		-542.36	0.19	0.18	-542.35	-0.01	-554.66	0.62	0.21	-554.26	-0.32
Ti-Ir		-543.35	0.19	0.16	-543.33	-0.03	-555.62	0.60	0.25	-555.27	-0.44
Ti-Rh		-542.09	0.19	0.16	-542.06	-0.21	-554.34	0.60	0.25	-553.98	-0.43
Ti-Ni		-540.83	0.19	0.16	-540.80	-1.06	-553.13	0.61	0.24	-552.77	-1.09
Ti-Cu		-537.65	0.19	0.17	-537.64	-0.88	-549.94	0.60	0.18	-549.52	-1.13
Ti-Zn		-535.32	0.18	0.18	-535.31	-0.36	-547.61	0.63	0.18	-547.16	-0.95
Ti-Ga		-537.04	0.19	0.16	-537.02	0.18	-549.46	0.64	0.16	-548.98	-0.48
		$E^*_{HCOOH}$	$E_{ZPE}$	TS	$G$	$\Delta G$					
Ti-Fe		-558.71	0.93	0.29	-558.07	0.73					
Ti-Co		-557.55	0.93	0.27	-556.89	0.82					
Ti-Ir		-558.60	0.93	0.25	-557.92	0.79					
Ti-Rh		-557.33	0.93	0.26	-556.65	0.78					
Ti-Ni		-555.95	0.93	0.25	-555.27	0.95					
Ti-Cu		-552.79	0.93	0.24	-552.10	0.87					
Ti-Zn		-550.44	0.93	0.25	-549.76	0.85					
Ti-Ga		-552.07	0.91	0.18	-551.34	1.09					
		$E^*_{H}$	$E_{ZPE}$	TS	$G$	$\Delta G$	$E^*_{H_2}$	$E_{ZPE}$	TS	$G$	$\Delta G$
Ti-Fe		-531.15	0.15	0.02	-531.02	0.07	-534.40	0.29	0.11	-534.22	0.25
Ti-Co		-529.99	0.15	0.02	-529.86	0.03	-533.19	0.31	0.13	-533.01	0.29
Ti-Ir		-530.94	0.15	0.02	-530.81	0.11	-534.23	0.32	0.17	-534.09	0.17
Ti-Rh		-529.61	0.15	0.02	-529.48	0.17	-532.96	0.32	0.17	-532.82	0.11
Ti-Ni		-528.56	0.16	0.02	-528.43	-0.16	-531.58	0.31	0.14	-531.41	0.46
Ti-Cu		-525.37	0.15	0.02	-525.24	-0.14	-528.40	0.31	0.14	-528.23	0.46

Ti-Zn	-523.02	0.15	0.02	-522.89	-0.14	-526.06	0.30	0.16	-525.92	0.41
Ti-Ga	-524.91	0.15	0.02	-524.78	-0.46	-527.64	0.31	0.20	-527.53	0.70

Table S14. The detailed electronic energy ( $E^*$ ), zero-point energy ( $E_{ZPE}$ ), entropy corrections (TS), free energy ( $G$ ), and Gibbs free energy change ( $\Delta G$ ) of critical intermediate in Cr-based heteronuclear BACs during electrochemical CO<sub>2</sub>RR towards C1 product and competitive HER product.

Species	$E^*$	$E^*_{CO_2}$	$E_{ZPE}$	TS	$G$	$\Delta G$	$E^*_{COOH}$	$E_{ZPE}$	TS	$G$	$\Delta G$
Cr-Fe	-528.49	-551.91	0.32	0.15	-551.73	-0.03	-555.26	0.64	0.15	-554.77	0.16
Cr-Co	-527.53	-550.63	0.32	0.25	-550.56	0.18	-553.45	0.64	0.16	-552.97	0.78
Cr-Ir	-528.42	-551.54	0.32	0.24	-551.46	0.17	-554.57	0.63	0.22	-554.16	0.50
Cr-Rh	-527.15	-550.26	0.32	0.23	-550.17	0.19	-553.11	0.63	0.21	-552.70	0.67
Cr-Ni	-525.56	-548.65	0.32	0.25	-548.58	0.19	-550.63	0.57	0.23	-550.29	1.49
Cr-Cu	-522.30	-545.38	0.32	0.22	-545.28	0.23	-547.75	0.62	0.17	-547.30	1.17
Cr-Zn	-519.81	-542.89	0.31	0.19	-542.77	0.25	-546.09	0.63	0.17	-545.63	0.34
Cr-Ga	-521.52	-544.65	0.32	0.15	-544.49	0.24	-548.38	0.60	0.20	-547.98	-0.29
		$E^*_{CO}$	$E_{ZPE}$	TS	$G$	$\Delta G$	$E^*_{HCOO}$	$E_{ZPE}$	TS	$G$	$\Delta G$
Cr-Fe		-544.63	0.21	0.12	-544.54	-0.65	-555.99	0.62	0.19	-555.55	-0.37
Cr-Co		-543.49	0.35	0.23	-543.37	-1.28	-554.40	0.61	0.15	-553.94	0.06
Cr-Ir		-544.41	0.19	0.10	-544.32	-1.05	-555.23	0.60	0.17	-554.80	0.10
Cr-Rh		-543.12	0.14	0.23	-543.21	-1.40	-553.98	0.61	0.22	-553.59	0.03
Cr-Ni		-541.52	0.14	0.18	-541.57	-2.17	-552.52	0.61	0.21	-552.12	-0.09
Cr-Cu		-538.29	0.15	0.19	-538.33	-1.91	-549.32	0.63	0.16	-548.84	-0.11
Cr-Zn		-535.88	0.15	0.22	-535.96	-1.22	-547.44	0.64	0.17	-546.97	-0.76
Cr-Ga		-537.47	0.15	0.18	-537.49	-0.40	-549.59	0.64	0.16	-549.11	-1.18
		$E^*_{HCOOH}$	$E_{ZPE}$	TS	$G$	$\Delta G$					
Cr-Fe		-558.75	0.94	0.22	-558.03	0.97					
Cr-Co		-557.62	0.91	0.27	-556.97	0.42					
Cr-Ir		-558.55	0.91	0.26	-557.90	0.35					
Cr-Rh		-557.27	0.91	0.27	-556.62	0.41					
Cr-Ni		-555.62	0.91	0.20	-554.91	0.66					
Cr-Cu		-552.40	0.90	0.22	-551.72	0.57					
Cr-Zn		-549.98	0.91	0.20	-549.28	1.14					
Cr-Ga		-551.81	0.91	0.10	-551.01	1.55					
		$E^*_{H}$	$E_{ZPE}$	TS	$G$	$\Delta G$	$E^*_{H_2}$	$E_{ZPE}$	TS	$G$	$\Delta G$
Cr-Fe		-532.04	0.19	0.01	-531.87	0.07	-535.37	0.30	0.16	-535.23	0.08
Cr-Co		-530.88	0.20	0.01	-530.69	0.29	-534.28	0.30	0.14	-534.11	0.03
Cr-Ir		-531.81	0.19	0.01	-531.63	0.24	-535.18	0.32	0.17	-535.03	0.05
Cr-Rh		-530.53	0.19	0.01	-530.35	0.25	-533.91	0.32	0.17	-533.76	0.03

Cr-Ni	-528.89	0.20	0.01	-528.71	0.30	-532.30	0.28	0.10	-532.13	0.03
Cr-Cu	-525.65	0.19	0.01	-525.47	0.28	-529.05	0.28	0.09	-528.86	0.06
Cr-Zn	-523.21	0.19	0.01	-523.03	0.23	-526.49	0.32	0.10	-526.27	0.20
Cr-Ga	-524.66	0.19	0.01	-524.48	0.49	-528.27	0.29	0.12	-528.11	-0.18

Table S15. The detailed electronic energy ( $E^*$ ), zero-point energy ( $E_{ZPE}$ ), entropy corrections (TS), free energy ( $G$ ), and Gibbs free energy change ( $\Delta G$ ) of critical intermediate in Mn-based heteronuclear BACs during electrochemical CO<sub>2</sub>RR towards C1 product and competitive HER product.

Species	$E^*$	$E^*_{CO_2}$	$E_{ZPE}$	TS	$G$	$\Delta G$	$E^*_{COOH}$	$E_{ZPE}$	TS	$G$	$\Delta G$
Mn-Fe	-528.19	-551.38	0.39	0.15	-551.14	0.26	-554.77	0.61	0.16	-554.33	0.01
Mn-Co	-526.94	-550.04	0.32	0.24	-549.96	0.19	-552.72	0.62	0.17	-552.27	0.88
Mn-Ir	-527.81	-550.92	0.32	0.24	-550.83	0.18	-553.73	0.63	0.16	-553.26	0.77
Mn-Rh	-526.56	-549.67	0.32	0.23	-549.58	0.19	-552.32	0.62	0.17	-551.87	0.91
Mn-Ni	-524.73	-547.83	0.32	0.24	-547.76	0.18	-549.94	0.59	0.18	-549.54	1.41
Mn-Cu	-521.57	-544.67	0.32	0.23	-544.58	0.20	-546.68	0.58	0.20	-546.30	1.48
Mn-Zn	-519.20	-542.30	0.31	0.19	-542.17	0.23	-545.34	0.60	0.19	-544.93	0.44
Mn-Ga	-521.30	-544.41	0.32	0.24	-544.34	0.17	-548.00	0.61	0.19	-547.58	-0.04
		$E^*_{CO}$	$E_{ZPE}$	TS	$G$	$\Delta G$	$E^*_{HCOO}$	$E_{ZPE}$	TS	$G$	$\Delta G$
Mn-Fe		-544.11	0.29	0.07	-543.90	-0.46	-554.54	0.60	0.17	-554.11	0.48
Mn-Co		-542.77	0.22	0.13	-542.68	-1.29	-553.17	0.61	0.17	-552.72	0.68
Mn-Ir		-543.58	0.21	0.09	-543.46	-1.09	-554.01	0.61	0.22	-553.62	0.66
Mn-Rh		-542.38	0.22	0.14	-542.30	-1.32	-552.78	0.61	0.22	-552.40	0.63
Mn-Ni		-540.65	0.21	0.08	-540.51	-1.86	-551.21	0.61	0.22	-550.82	0.38
Mn-Cu		-537.38	0.23	0.07	-537.23	-1.82	-547.96	0.61	0.14	-547.49	0.54
Mn-Zn		-535.04	0.20	0.03	-534.87	-0.82	-545.71	0.63	0.18	-545.26	0.36
Mn-Ga		-537.05	0.23	0.08	-536.90	-0.21	-547.88	0.63	0.18	-547.43	0.36
		$E^*_{HCOOH}$	$E_{ZPE}$	TS	$G$	$\Delta G$					
Mn-Fe		-558.42	0.91	0.26	-557.77	-0.21					
Mn-Co		-557.07	0.91	0.28	-556.44	-0.27					
Mn-Ir		-557.95	0.91	0.27	-557.32	-0.25					
Mn-Rh		-556.73	0.91	0.26	-556.07	-0.23					
Mn-Ni		-554.86	0.91	0.22	-554.17	0.10					
Mn-Cu		-551.74	0.94	0.23	-551.04	-0.10					
Mn-Zn		-549.42	0.91	0.27	-548.77	-0.07					
Mn-Ga		-551.49	0.92	0.18	-550.76	0.12					
		$E^*_{H}$	$E_{ZPE}$	TS	$G$	$\Delta G$	$E^*_{H_2}$	$E_{ZPE}$	TS	$G$	$\Delta G$
Mn-Fe		-531.49	0.20	0.01	-531.29	0.34	-535.03	0.32	0.17	-534.89	-0.15
Mn-Co		-530.14	0.20	0.01	-529.94	0.44	-533.68	0.29	0.05	-533.45	-0.06

Mn-Ir	-531.01	0.20	0.01	-530.81	0.44	-534.56	0.29	0.05	-534.31	-0.05
Mn-Rh	-529.75	0.20	0.01	-529.56	0.45	-533.32	0.29	0.11	-533.14	-0.13
Mn-Ni	-528.01	0.20	0.01	-527.82	0.36	-531.49	0.30	0.04	-531.24	0.03
Mn-Cu	-524.75	0.20	0.01	-524.55	0.46	-528.19	0.35	0.05	-527.89	0.12
Mn-Zn	-522.38	0.13	0.01	-522.25	0.39	-525.96	0.29	0.13	-525.80	-0.09
Mn-Ga	-524.47	0.19	0.01	-524.29	0.46	-528.05	0.29	0.12	-527.89	-0.15

Table S16. The detailed electronic energy ( $E^*$ ), zero-point energy ( $E_{ZPE}$ ), entropy corrections (TS), and free energy ( $G$ ) of isolated molecule during electrochemical CO<sub>2</sub>RR towards C1 product and competitive HER product.

Species	$E^*$	$E_{ZPE}$	TS	$G$
CO <sub>2</sub>	-22.96	0.31	0.66	-23.21
CO	-14.84	0.14	0.61	-15.31
H <sub>2</sub> O	-14.25	0.59	0.58	-14.24
H <sub>2</sub>	-6.76	0.27	0.40	-6.89
HCOOH	-29.97	0.90	0.99	-30.06

In this work, we consider two coordination forms of BACs, i.e., 3-coordinated and 4-coordinated metal-anchored N-doped graphene, as shown in Fig. S1. We select three metals, Fe, Mn, and Mo, as the representative to compare the DFT energy of the different coordination forms. Due to the significantly lower energy of 4-coordinated form, thus all of our subsequent investigation are based on the 4-coordinated form of BACs.



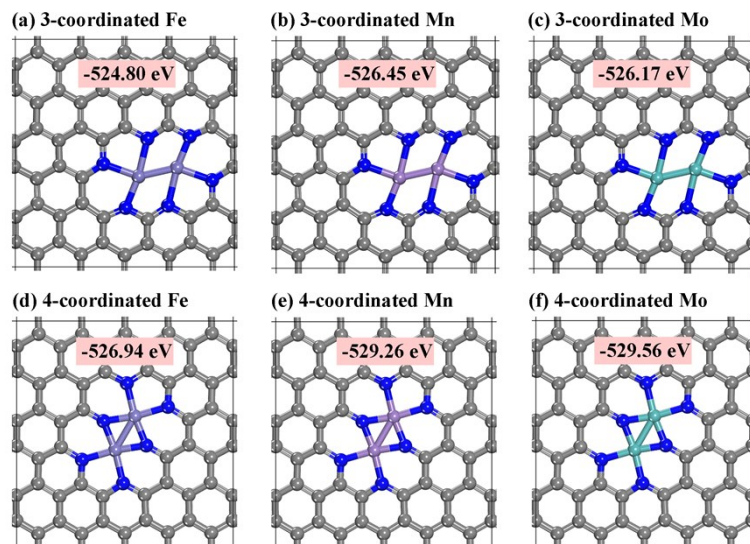


Fig. S1 The most stable structures and the DFT energy of 3-coordinated and 4-coordinated metal-anchored N-doped graphene homonuclear BACs.

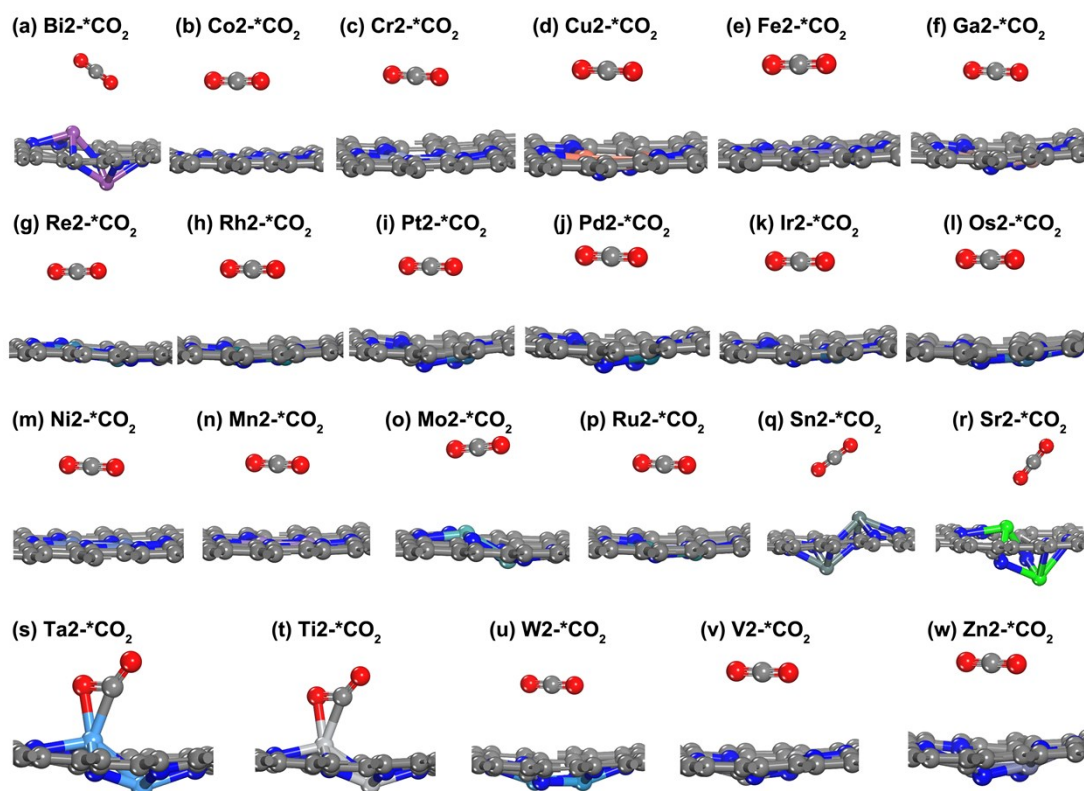


Fig. S2 The most stable structures of \*CO<sub>2</sub> adsorbed on 23 kinds of homonuclear BACs.

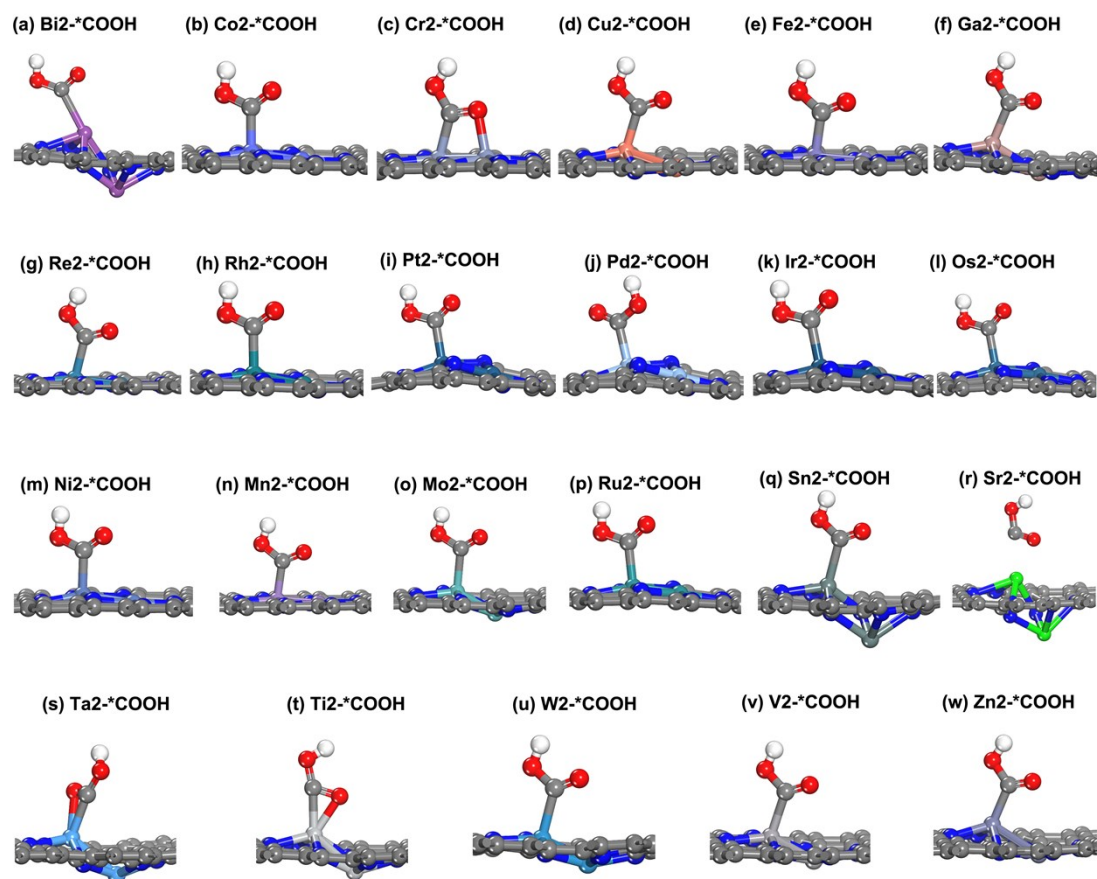


Fig. S3 The most stable structures of \*COOH adsorbed on 23 kinds of homonuclear BACs.

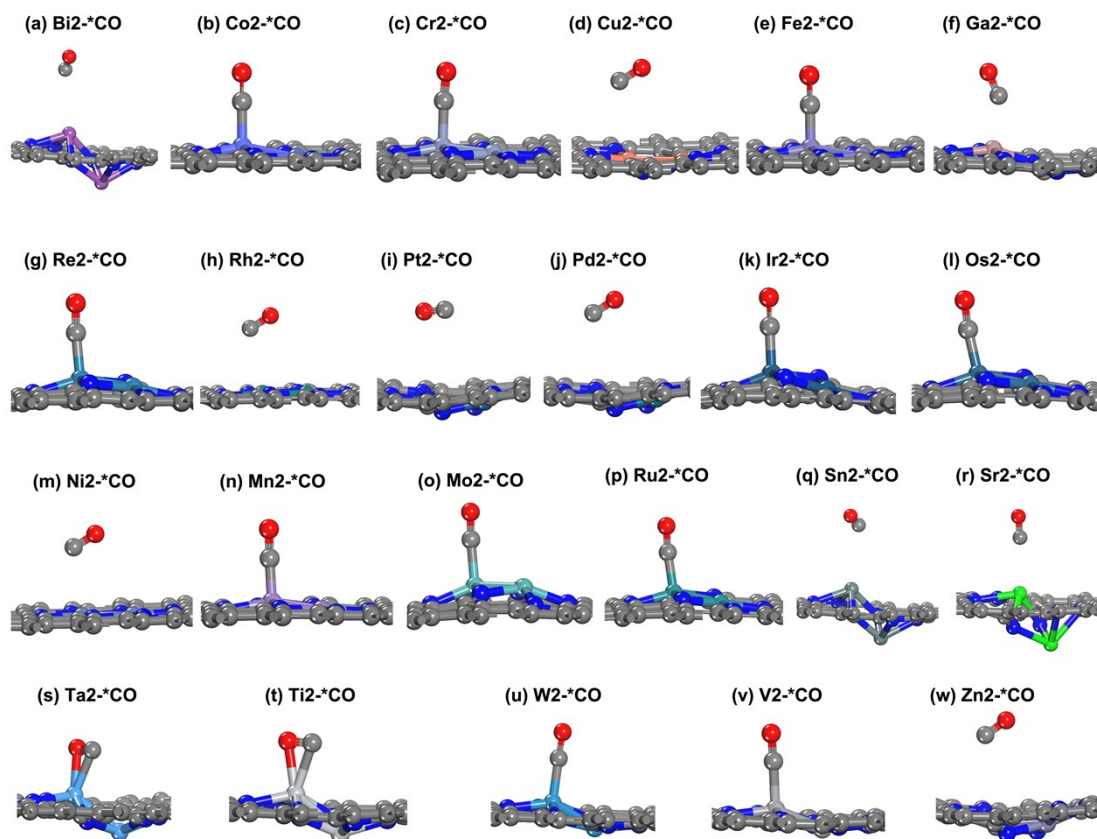


Fig. S4 The most stable structures of \*CO adsorbed on 23 kinds of homonuclear BACs.

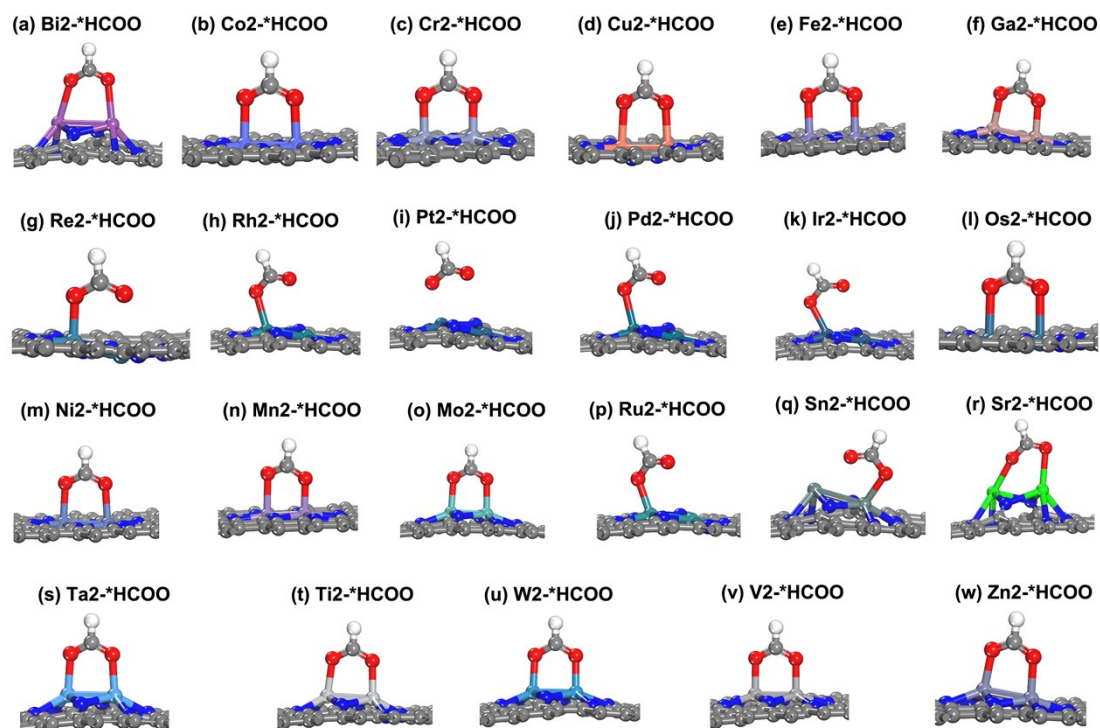


Fig. S5 The most stable structures of \*HCOO adsorbed on 23 kinds of homonuclear

BACs.

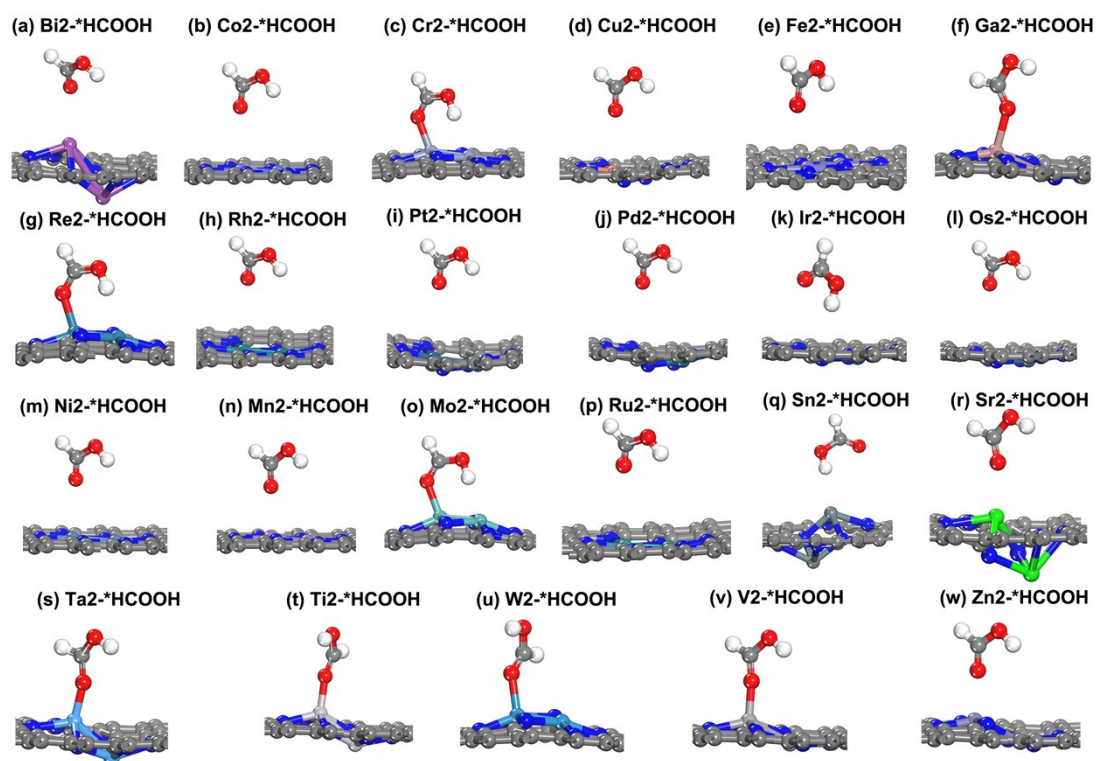


Fig. S6 The most stable structures of \*HCOOH adsorbed on 23 kinds of homonuclear BACs.

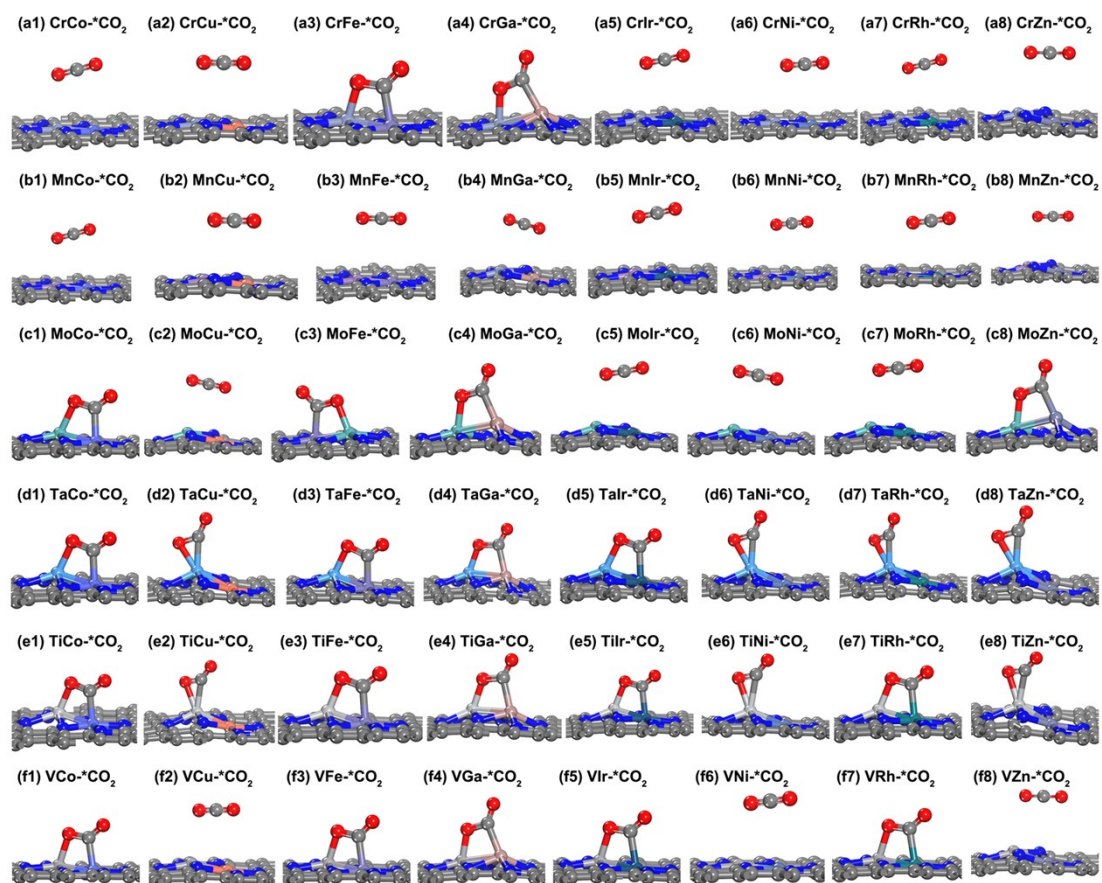


Fig. S7 The most stable structures of \*CO<sub>2</sub> adsorbed on 48 kinds of heteronuclear BACs.

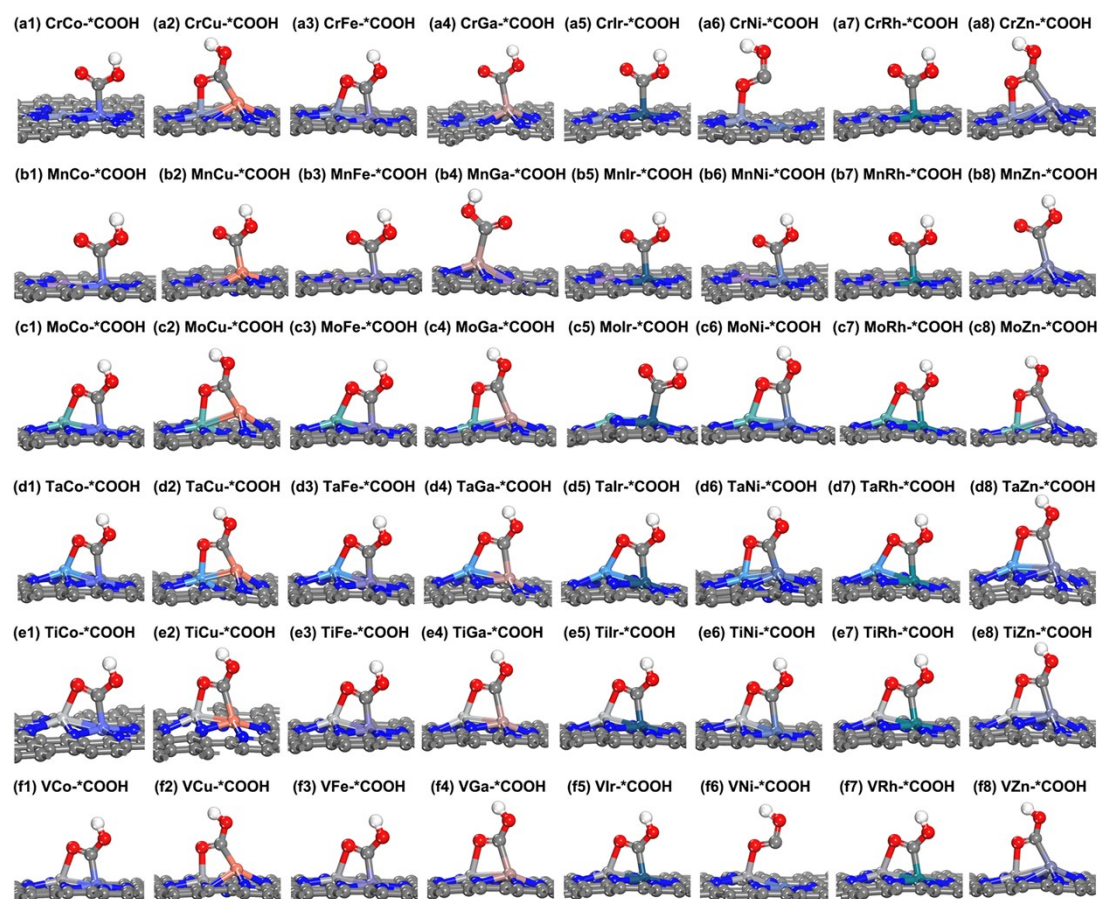


Fig. S8 The most stable structures of \*COOH adsorbed on 48 kinds of heteronuclear BACs.

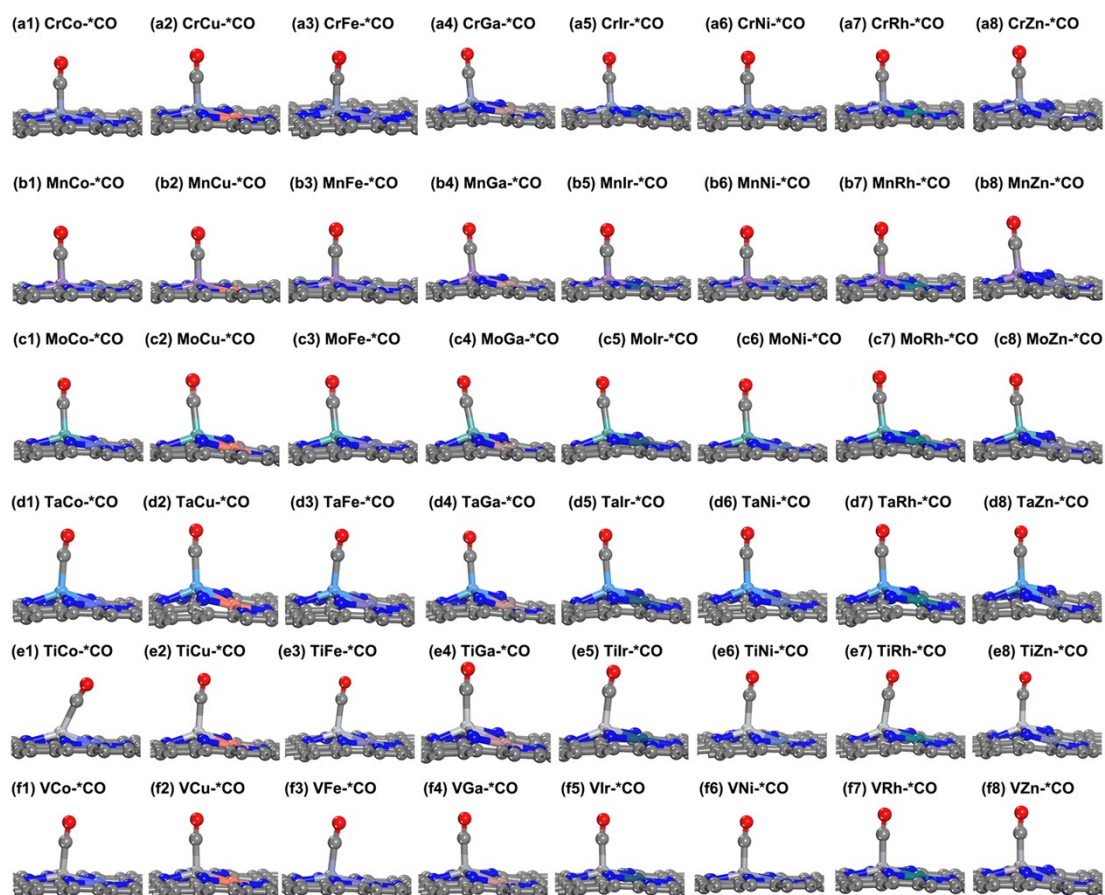


Fig. S9 The most stable structures of \*CO adsorbed on 48 kinds of heteronuclear BACs.

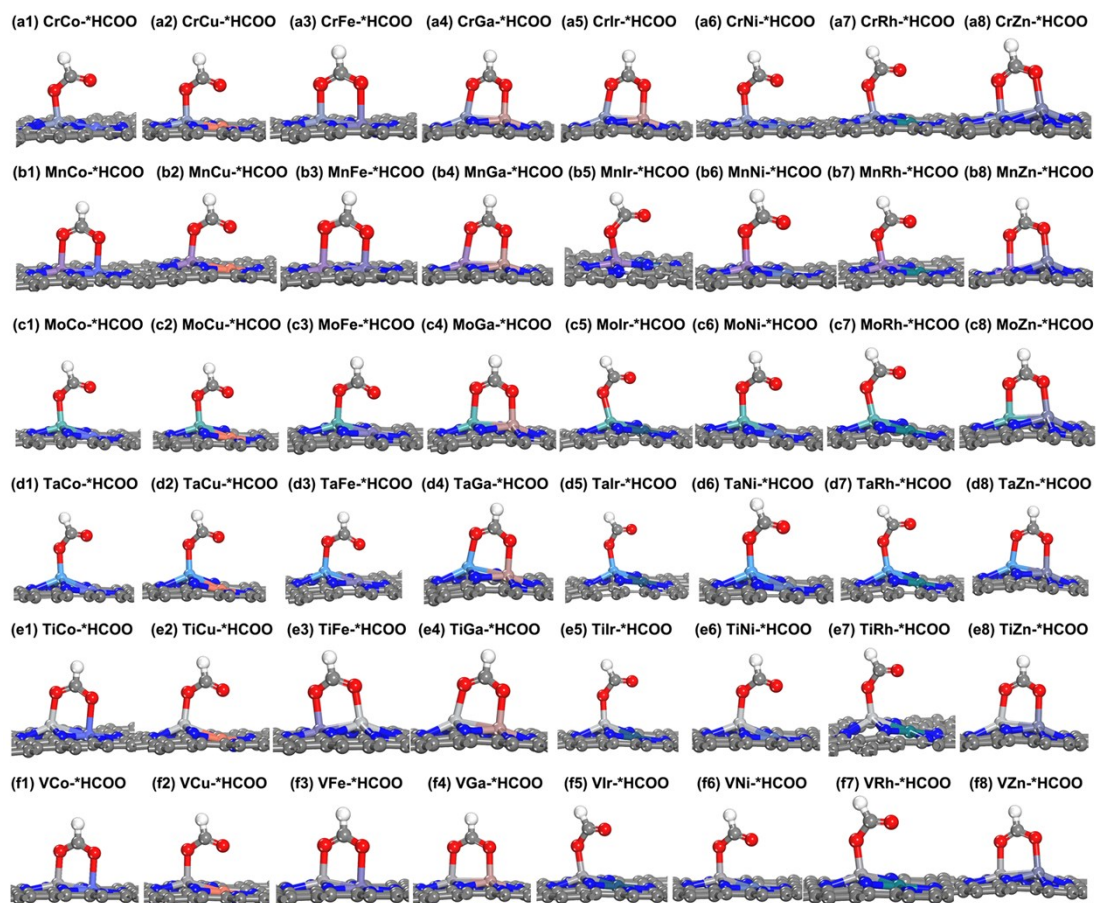


Fig. S10 The most stable structures of \*HCOO adsorbed on 48 kinds of heteronuclear BACs.



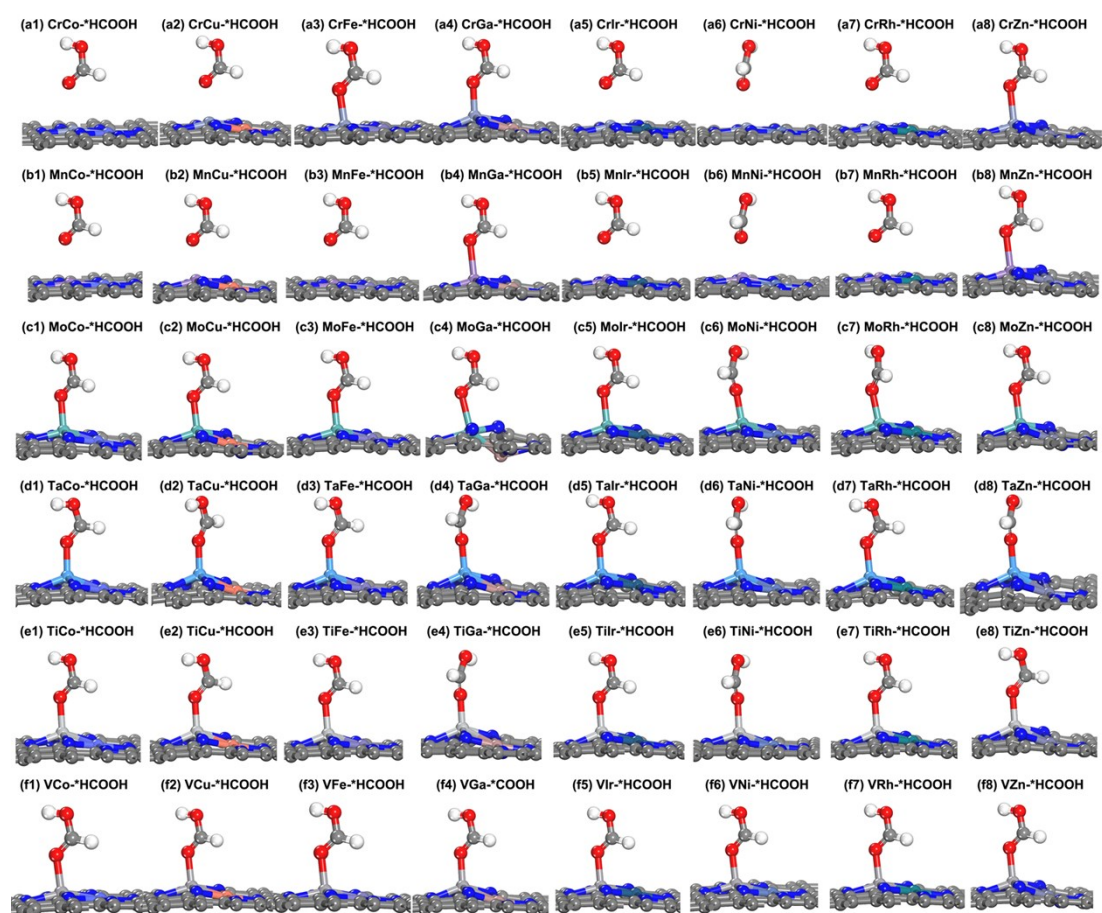


Fig. S11 The most stable structures of \*HCOOH adsorbed on 48 kinds of heteronuclear BACs.

## REFERENCES

1. X. Y. Guo, J. X. Gu, S. R. Lin, S. L. Zhang, Z. F. Chen and S. P. Huang, *J. Am. Chem. Soc.*, 2020, **142**, 5709-5721.